

Research Article



Meterocycles Very Important Paper

How to cite: Angew. Chem. Int. Ed. 2025, e17656 doi.org/10.1002/anie.202517656

One Collision – Two Heteroatoms: Gas-Phase Preparation of Azasilabenzenes

Surajit Metya, Iakov A. Medvedkov, Shane J. Goettl, Tosaporn Sattasathuchana,* Mateus X. Silva, Breno R. L. Galvão,* and Ralf I. Kaiser*

Abstract: Nature has long favored cyclic, particularly heterocyclic, molecules in the synthesis of key biomolecules. Siliconsubstituted hydrocarbons have gained increasing attention due to their unique chemical bonding and electronic structure compared to their iso-valent carbon counterparts. However, the synthesis of silicon-containing heterocyclic molecules remains a significant challenge. In this work, we investigate the reaction mechanism leading to a sparsely explored class of silicon- and nitrogen-containing aromatic heterocycles, in which silicon and nitrogen atoms are positioned adjacently within an aromatic, six-membered ring: azasilabenzenes. This is achieved through the reaction of the silicon nitride (SiN) radical with 1,3-butadiene (C_4H_6) via single collision conditions, exploiting a crossed molecular beam experiment combined with electronic structure calculations and statistical analysis. Our results reveal the formation of two novel cyclic products: 1-aza-2-silacyclohexa-3,5-dien-2-ylidene and 1-aza-2-silabenzene. Interestingly, this reaction contrasts with the iso-valent system involving the cyano radical (CN) and 1,3-butadiene (C_4H_6), which predominantly yields an acyclic product (1-cyano-1,3-butadiene) via a simple addition-elimination pathway. In addition to elucidating the reaction pathways, this study also provides insights into the nature of bonding and atomic interactions in the resulting products, offering a deeper understanding of structure–stability relationships in silicon–nitrogen heterocycles and the counterintuitive concept of iso-valency.

Introduction

Heterocyclic organic molecules are characterized by cyclic moieties where one or more carbon atoms are substituted by heteroatoms, commonly nitrogen (N), oxygen (O), sulfur (S), or silicon (Si).^[1-3] These rings can be saturated, unsaturated, or aromatic and play a fundamental role in natural products like amino acids (1–3)^[4,5] and vitamins (4–9),^[5] pharmaceuticals such as Clonidine, Temazepam, and Alprazolam (10–15),^[6-9] and biologically essential compounds serving critical functions in cellular metabolism and as genetic materials like purine (16) and pyrimidine (17) bases in deoxyribonucleic acid (DNA) (Scheme 1).^[10] Over the

number of valence electrons and hence, are iso-valent. This "carbon–silicon switch" invokes Langmuir's concept of iso-valency, which predicts similarities in structural and chemical properties.^[11] This perception captivated the attention of both the synthetic and theoretical chemistry communities from the fundamental point of view of the reactivity, stability, chemical bonding, and electronic structure of exotic organosilicon molecules (Scheme 2).^[12–16]

However, experimental findings revealed that Lang-

last decade, silicon-substituted heterocyclic molecules have received special attention as carbon and silicon share the same

However, experimental findings revealed that Langmuir's iso-valency concept is not always as predictive as expected.[17,18] While acetylene (C₂H₂) is the most stable isomer on the C₂H₂ potential energy surface (PES), with the vinylidene ($H_2C=C$) isomer less stable by 291 kJ mol⁻¹, the replacement of one carbon atom by silicon results in the silavinylidene isomer (H₂C=Si) as the global minimum. [18-20] Furthermore, when both carbon atoms are replaced by silicon, a double-bridged butterfly structure disilyne (Si(μ-H₂)Si) represents a local minimum on the Si₂H₂ potential energy surface.^[21,22] The primary reason for this divergence arises from the larger atomic radius of silicon (110 pm) compared to carbon (70 pm), its lower electronegativity (1.90 vs. 2.55 on the Pauling scale), and the less effective sp mixing between the 3s and 3p orbitals relative to the 2s and 2p orbitals. Comparing the 6π aromatic benzene molecule $(C_6H_6, 21)$ with silabenzene $(SiC_5H_6, 23)$, this results in longer silicon-carbon bond lengths of about 177 pm in 23 versus 140 pm for the carbon-carbon bond in 21.[23-25] These distinct molecular properties upon silicon substitution

[*] Dr. S. Metya, Dr. I. A. Medvedkov, S. J. Goettl, Dr. T. Sattasathuchana, Prof. Dr. R. I. Kaiser Department of Chemistry, University of Hawai'i at Manoa, Honolulu, Hawaii 96822, USA

E-mail: tsatta@hawaii.edu ralfk@hawaii.edu

Dr. M. X. Silva, Dr. B. R. L. Galvão Centro Federal de Educação Tecnológica de Minas Gerais, Belo Horizonte 30421-169, Brazil E-mail: brenogalvao@gmail.com

Dr. M. X. Silva

Present address: Departamento de Química, Universidade Federal de Ouro Preto, Campus Morro do Cruzeiro, Ouro Preto, Minas Gerais 35402-136, Brazil

Additional supporting information can be found online in the Supporting Information section

15213773, 0, Downloaded from https://onlinelibrary.wiley.com/doi/10.1002/anie.202517656 by University Of Hawaii At Manoa, Wiley Online Library on [10/11/2025]. See the Terms and Conditions (https://onlinelibrary.wiley.com/

and-conditions) on Wiley Online Library for rules of use; OA articles are governed by the applicable Creative Commons License

Scheme 1. Heterocycles present in amino acid, vitamin, drug, and genetic molecules.

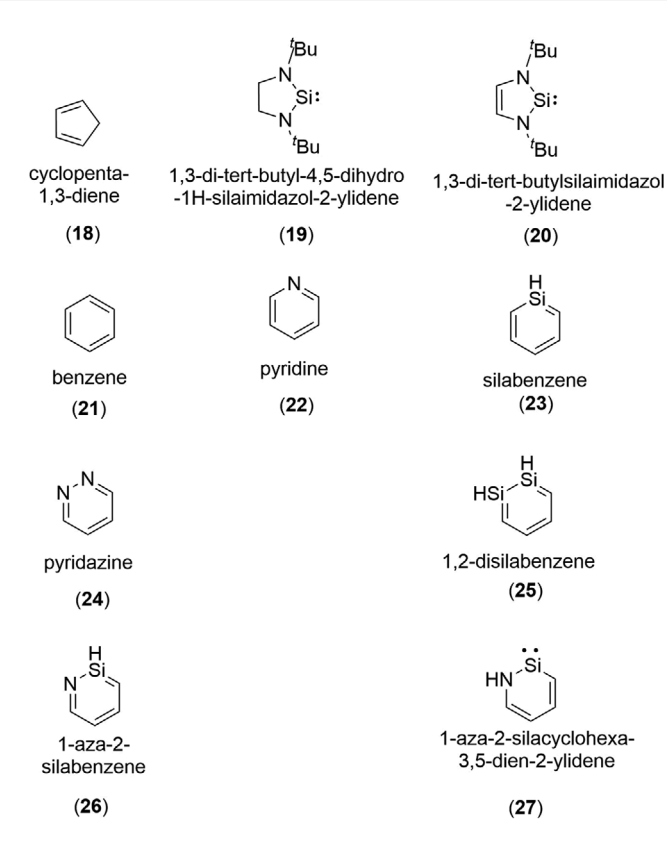
not only enable the design of iso-valent, nontoxic variants such as ibuprofen versus sila-ibuprofen, [26] but also provide environmentally friendly organosilicon counterparts like silicon-based fertilizer. [27,28] Therefore, innovative silicon heterocycles have received particular attention as building blocks of conjugated π -systems owing to their electroluminescence

and highly efficient electron transportation at the molecular level. $^{[29]}$

Disubstituted heterocycles with adjacent nitrogen and silicon atoms have garnered special focus considering their aptitude of forming stable divalent silylenes (SiR₂)—silicon analogs of carbenes (CR₂)—in the singlet state.^[30,31] This

15213773, 0, Downloaded from https://onlinelibrary.wiley.com/doi/10.1002/anie.202517656 by University Of Hawaii At Manoa, Wiley Online Library on [10/11/2025]. See the Terms and Conditions (https://onlinelibrary.wiley.com/emrs/

and-conditions) on Wiley Online Library for rules of use; OA articles are governed by the applicable Creative Commons License



Scheme 2. Structure of the five and six-membered heterocyclic molecules with silicon and/or nitrogen substitution.

stability arises from the donation of the lone pair of electrons from the nitrogen to the empty 3p orbitals of the silicon atom.[32] However, while five-membered nitrogen heterocyclic silylenes such as 1,3-di-tert-butyl-4,5-dihydro-1H-silaimidazol-2-ylidene (19) and 1,3-di-tertbutylsilaimidazol-2-ylidene (20) have been extensively investigated both experimentally and theoretically with stable, even "bottleable" compounds successfully synthesized (Scheme 2), [33-36] the synthesis of six-membered nitrogen heterocyclic silvlenes has provided a fundamental synthetic challenge to the preparative organic chemistry community, and hence, only a few computational studies have been reported in the literature.[37] Veszprémi et al. investigated six-membered nitrogen-containing heterocyclic silylenes (SiNC₄H₅)—isovalent molecules of benzene (C₆H₆, 21)—computationally.^[38] Although fully valence saturated and 6π Hückel aromatic, the 1-aza-2-silabenzene (26) isomer is less stable by 36-48 kJ mol⁻¹ compared to the silylene-type isomer 1-aza-2-silacyclohexa-3,5-dien-2-ylidene (27). This observation parallels the stabilities observed in acyclic systems, where the silylene-type isomer aminosilylene (HSi-NH₂) exhibits a stabilization energy of 58 kJ mol⁻¹ compared to the silaimine (H₂Si=NH) isomer. [39,40] This finding is particularly intriguing since pyridazine (24) and 1,2-disilabenzene (25), which contain two adjacent nitrogen and silicon heteroatoms, respectively, exhibit aromatic behavior.[14,41] However, despite their intriguing chemical bonding and molecular structure, an experimental preparation of six-membered silvlene molecules featuring adjacent

nitrogen and silicon atoms has not vet been accomplished. thus classifying azasilabenzenes as one of the least explored classes of organosilicon chemistry.

Here, we report the first gas-phase synthesis of two six-membered, silicon-nitrogen heterocyclic counterparts of benzene (C₆H₆, 21)—1-aza-2-silabenzene (26) and 1-aza-2-silacyclohexa-3,5-dien-2-vlidene (27). This preparation is accomplished via a gas-phase reaction of ground-state silicon nitride radicals (SiN, $X^2\Sigma^+$) with 1,3-butadiene (C₄H₆, X^1A_{α}) under single collision conditions, exploiting the crossed molecular beams approach. In strong contrast to a classical preparative synthesis, in crossed molecular beam experiments, both reactants can be prepared in separate source chambers in distinct molecular beams.[42-45] The nascent reaction products then "fly away" undisturbed from the collision center prior to their detection in a differentially pumped quadrupole mass spectrometer. Therefore, this investigation on the molecular level, supported by electronic structure calculations, offers a fundamental understanding of the reaction dynamics in an isolated environment, which is free from wall effects and secondary collisions, thus affording a "clean" and selective synthesis of two novel siliconnitrogen heterocyclic molecules: 1-aza-2-silabenzene (26) and 1-aza-2-silacyclohexa-3,5-dien-2-ylidene (27) (reaction (1)). Unlike the reaction of 1,3-butadiene (C₄H₆, X¹A₂) with the isovalent cyano radical (CN, $X^2\Sigma^+$), which favors the preparation of acyclic products like 1-cyano-1,3-butadiene over pyridine, [46,47] the reaction of silicon nitride radicals (SiN, $X^2\Sigma^+$) and 1,3-butadiene (C₄H₆, X^1A_9) yields exclusively cyclic products. Hence, this system is stimulating from the viewpoint of a physical-organic chemist as such compounds represent benchmarks to unravel the chemical reactivity, bond-breaking processes, and synthesis of cyclic organosilicon molecules from acyclic precursors, thereby opening new avenues to the rather obscure class of silicon-nitrogen containing heterocyclic molecules: azasilabenzenes.

$$SiN + C_4H_6 \rightarrow SiNC_4H_5 + H \tag{1}$$

Results and Discussion

Laboratory Frame

The experiments were carried out under single-collision conditions employing a crossed molecular beams machine.[42,43,45,48] Reactive scattering signals for the bimolecular reaction between ground-state silicon nitride radical (SiN, $C_{\infty v}$, $X^2\Sigma^+$) and 1,3-butadiene (C_4H_6 , C_{2h} , X^1A_g) were recorded at a mass-to-charge ratio (m/z) of 95 (Figure 1). Considering the natural abundance of the isotopes of carbon [12C (98.9%), 13C (1.1%)] and silicon [28 Si (92.2%), 29 Si (4.7%), 30 Si (3.1%)], signal at m/z = 95may correspond to ²⁸SiN¹²C₄H₅, ²⁸SiN¹³C¹²C₃H₄, and/or ²⁹SiN¹²C₄H₄ accompanied by atomic hydrogen and molecular hydrogen losses, respectively. It should be emphasized that under our experimental conditions, no reactive scattering signal was observed at m/z = 94 (28 SiN 12 C₄H₄), which would

15213773, 0. Downloaded from https://oninelibrary.wile.com/doi/10.1002/anie.202517656 by University Of Hawaii At Manoa, Wiley Online Library on 10/11/2025]. See the Terms and Conditions (https://onlinelibrary.wiley.com/com/terms-and-conditions) on Wiley Online Library for rules of use; OA articles are governed by the applicable Creative Commons Licenses

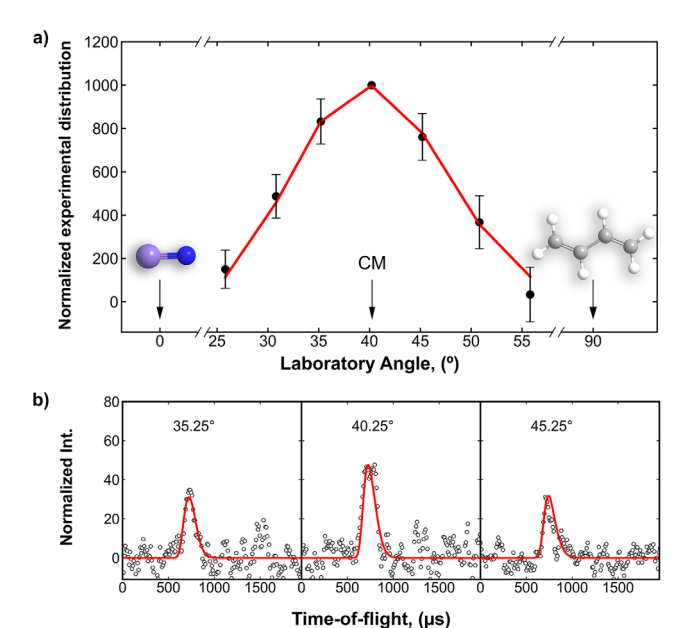


Figure 1. a) Laboratory angular distribution and b) time-of-flight (TOF) spectra recorded at m/z=95 for the reaction involving silicon nitride (SiN, $C_{\infty v}$, $X^2\Sigma^+$) and 1, 3 butadiene (C_4H_6 , C_{2h} , X^1A_1). In a), the solid circles with error bars represent the normalized experimental distribution with $\pm 1\sigma$ uncertainty (standard deviation of the TOF integrals for each angle), while in b), the experimental data are shown as open black circles. For each angle, 1.5×10^6 TOF spectra (15 h total acquisition) were averaged to achieve an adequate signal-to-noise ratio. The red solid lines in a) and b) correspond to the best-fit results from the forward-convolution routine. Atoms are color-coded in blue (nitrogen), violet (silicon), grey (carbon), and white (hydrogen).

correspond to the molecular hydrogen loss (H2) channel. This observation alone confirms that the reaction between silicon nitride radical (SiN, $C_{\infty v}$, $X^2\Sigma^+$) and 1,3-butadiene (C₄H₆, C_{2h}, X¹A_g) yields a product with the chemical formula ²⁸SiN¹²C₄H₅ formed via reaction (1) through atomic hydrogen loss. Time-of-flight (TOF) spectra were then recorded at m/z = 95 at laboratory angles from 25.25° to 55.25° in 5° intervals, scaled, and integrated to obtain the laboratory angular distribution (LAD). This LAD is spread over 30° in the scattering plane defined by both beams (Figure 1) and peaks at the center-of-mass angle of 40.25°. The ion signal in the TOF spectra was spread over some 250 µs, ranging from 600 to 850 µs. Overall, the laboratory data suggest the exclusive gas-phase preparation of SiNC₄H₅ isomer(s) via the elementary gas-phase reaction of the silicon nitride radical (SiN, $C_{\infty v}$, $X^2\Sigma^+$) with 1,3-butadiene (C_4H_6 , C_{2h} , X^1A_g).

Center-of-Mass Frame

Having provided compelling evidence on the gas-phase synthesis of the previously elusive SiNC₄H₅ isomer(s), our ultimate goal is to identify the nature of the isomer(s) formed and also aim to unravel the most likely reaction pathways. This is accomplished by transforming the experimental data from the laboratory (LAB) to the center-of-mass

(CM) reference frame by exploiting a forward-convolution technique.[49,50] Figure 2 presents the translational energy flux distribution, $P(E_T)$, and the angular flux distribution, $T(\theta)$, in the CM frame corresponding to the best fit of the experimental data. The most comprehensive representation of the reaction dynamics is provided by the product flux contour map, which depicts the reactive differential cross section in terms of intensity as a function of scattering angle θ and CM velocity u, $\mathbf{I}(\theta, u)$, where $\mathbf{I}(\theta, u) \sim \mathbf{P}(u) \times \mathbf{T}(\theta)$. To elucidate the underlying reaction dynamics, analysis of the $P(E_T)$ offers several key insights. First, when the product isomers exhibit well-separated energetics, the maximum translational energy (E_{max}) can be employed to identify the nature of the reaction products, since $E_{\rm max}$ is the sum of the reaction exoergicity and the experimental collision energy (E_c) for those molecules born without internal energy.^[51] Here, $E_{\rm max}$ is derived from the P($E_{\rm T}$) to be 170 \pm 42 kJ mol⁻¹. Considering the experimental collision energy of 24.0 ± 0.5 kJ mol⁻¹, the reaction exoergicity is thereby evaluated to be 147 \pm 42 kJ mol⁻¹. Second, the P(E_T) exhibits a plateau from 0 to approximately 30 kJ mol⁻¹, suggesting the involvement of both a loose exit channel, characterized by minimal changes in geometry and electron density, and a tight exit transition state, marked by substantial structural and electronic rearrangements, during the formation of the final SiNC₄H₅ products from the decomposing SiNC₄H₆ intermediates.^[42,48,52] Finally. the center-of-mass angular distribution, $T(\theta)$, provides further insight into the underlying reaction dynamics. It exhibits intensity over the complete angular range proposing indirect scattering dynamics. Further, this distribution is slightly backward scattered relative to the primary SiN beam, with an intensity ratio of $I(0^{\circ})/I(180^{\circ}) = (0.8 \pm 0.2)$: 1. This observation suggests that at least one reaction channel involves a relatively short-lived SiNC₄H₆ intermediate that ejects atomic hydrogen.^[52] These findings are also illustrated in the flux velocity-angle contour map (Figure 2c), which offers a comprehensive view of the scattering behavior in the reaction.

Electronic Structure Calculations and Reaction Mechanism

In case of polyatomic reactants, it is beneficial to combine the experimental data with electronic structure calculations. First, the nature of the SiNC₄H₅ structural isomer(s) can be determined by comparing the experimentally measured reaction exoergicity with the reaction energies of possible isomers obtained from electronic structure calculations. The geometries of the corresponding reactants, products, intermediates, and transition states are optimized at the B2PLYP-D3(BJ)/Def2-TZVPP^[53-57] level of theory; energies are refined exploiting CCSD(T)-F12/cc-pVTZ-F12^[58-61] (Supporting Information). This computational investigation revealed three atomic hydrogen loss reaction channels (p1-p3) leading to distinct SiNC₄H₅ isomers: 1-aza-2-silacyclohexa-3,5-dien-2-ylidene (p1, C_s, X¹A', -157 kJ mol^{-1}), 1-aza-2-silabenzene (**p2**, C_s, X¹A', -132 kJ mol^{-1}), and 1-silaisocyano-1,3-butadiene (p3, C_s, X¹A', -67 kJ mol^{-1}). The relative stability of the products **p1** and **p2** agrees

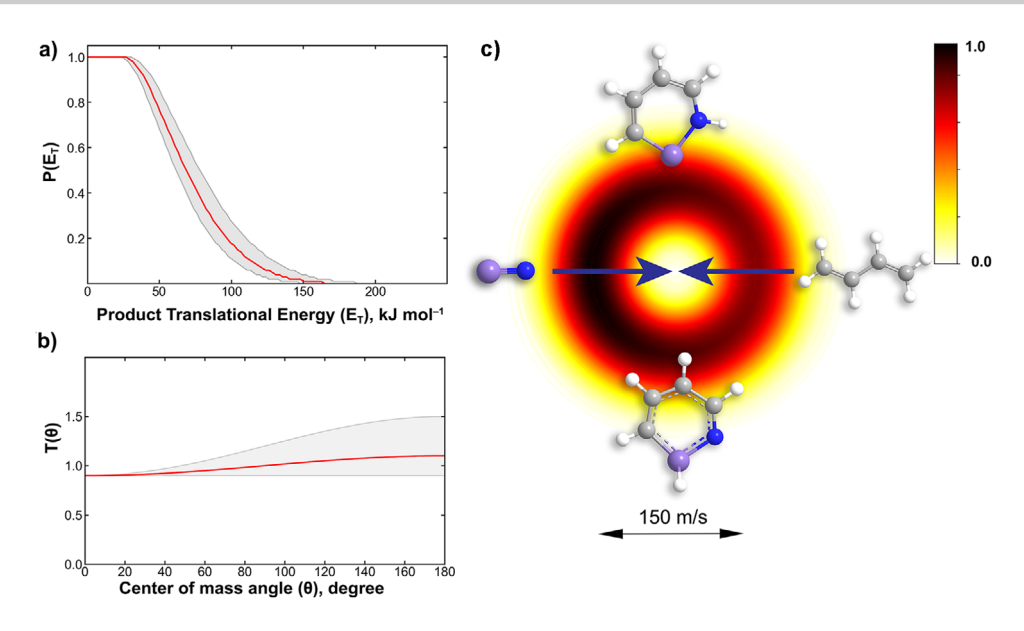


Figure 2. a) Center-of-mass translational energy distribution $P(E_T)$, b) the angular flux distribution $T(\theta)$, and c) the flux contour map (top view) leading to the formation silicon nitrogen containing heterocyclic products from the reaction between ground state silicon nitride radical (SiN, $C_{\infty v}$, $X^2 \Sigma^+$) and 1, 3 butadiene (C₄H₆, C_{2h}, X^1 A₁). The solid red lines indicate the best fit, while the shaded regions represent the error margins. The direction of the silicon nitride is defined by 0°, while that of the 1, 3 butadiene is at 180°. Atoms are color-coded in blue (nitrogen), violet (silicon), grey (carbon), and white (hydrogen).

well with a previous study by Veszprémi and coworkers^[38] where they also identified an isomerization pathway of **p2** to **p1** through a transition state of 200 kJ mol⁻¹. Nevertheless, this barrier is well above the total energy of our system, thus blocking the conversion from **p2** to **p1**. Our work also identified the existence of multiple intermediates (**i1-i6**) on the doublet potential energy surface and nine transition states (**TS1-TS9**).

The reaction is initiated without a barrier through the addition of the silicon nitride radical (SiN, $C_{\infty v},\, X^2\Sigma^+)$ with its nitrogen atom to the π -electron density of the terminal carbon atom of 1,3-butadiene (C_4H_6 , C_{2h} , X^1A_{α}) forming a carbon-nitrogen bond in the collision complex i1 (SiNC₄H₆, C_1 , X^2A); the latter is stabilized by 220 kJ mol⁻¹ with respect to separated reactants. The collision complex can either undergo atomic hydrogen elimination to the acyclic product silaisocyano-1,3-butadiene (SiNC₄H₅, **p3**, C_s, X¹A') via a transition state (TS1) with a barrier of 16 kJ mol⁻¹ with respect to p3 or isomerize to the s-cis conformer i2 (SiNC₄H₆, C₁, X²A) by overcoming a low barrier (TS2) of 61 kJ mol⁻¹; **i2** isomerizes to **i3** (SiNC₄H₆, C₈, X^2A') via ring closure. It is important to note the existence of an alternative path to i3 via the addition of the silicon nitride radical through the silicon atom, forming a silicon-carbon bond, followed by a cyclization to i3. However, these steps involve transition states well above the energy of the separated reactants and hence cannot be accessed at our experimental collision energy. From i3, the reaction can proceed via two competing pathways: one leads to intermediate **i4** (SiNC₄H₆, C_s, X²A") through a hydrogen migration from carbon to silicon; alternatively, intermediate i5 (SiNC₄H₆, C₁, X^2A) forms via hydrogen migration from the methylene moiety to the nitrogen atom. Intermediate i4 may either undergo

unimolecular decomposition to product $\mathbf{p2}$ via hydrogen atom elimination or undergo further hydrogen migration from carbon to nitrogen to yield $\mathbf{i6}$ (SiNC₄H₆, C₁, X²A). Alternatively, $\mathbf{i6}$ can also form in one step from $\mathbf{i5}$ through hydrogen migration from carbon to silicon. Intermediate $\mathbf{i6}$ can subsequently decompose through atomic hydrogen loss, either forming $\mathbf{p1}$ via a loose transition state or $\mathbf{p2}$ via a pathway with a barrier of 19 kJ mol⁻¹.

Among all possible pathways from reactants to products, the most probable one can be identified by comparing experimental observations with computational predictions. The experimentally derived exoergicity of the reaction is 147 \pm 42 kJ mol⁻¹, which agrees well with the computed reaction energies for both **p1** ($-157 \pm 15 \text{ kJ mol}^{-1}$) and **p2** (-132 \pm 15 kJ mol⁻¹). In contrast, the calculated exoergicity of the acyclic product p3 (-67 kJ mol⁻¹) is significantly less exoergic, thereby ruling out the $i1 \rightarrow TS1 \rightarrow p3$ pathway as a dominant channel. As shown in Figure 3, the transition state TS4 lies higher in energy than TS5, indicating that the intermediate i3 is more likely to isomerize to i5 rather than to i4. However, both transition states are below the energy of the separated reactants thus some fraction of the i3 intermediate may convert to **i4**, overcoming the transition state **TS4**. In this case, from i4, formation of the product p2 is more favorable as the transition state TS7 is lower in energy compared to the transition state of the isomerization step from $i4 \rightarrow i6$. On the other hand, from i5, two potential pathways emerge to the products p1 and p2: (a) i5 \rightarrow TS8 \rightarrow i6 \rightarrow p1, and (b) i5 \rightarrow TS8 \rightarrow i6 \rightarrow TS9 \rightarrow p2. The experimentally derived kinetic energy flux distribution shows a plateau from 0 to approximately 30 kJ mol⁻¹, indicating that both a barrierless decomposition of the i6 intermediate to p1 (path a) and hydrogen atom elimination via a tight exit transition aded from https://onlinelibrary.wiley.com/doi/10.1002/anie.2025/17656 by University Of Hawaii At Manoa, Wiley Online Library on [10/11/2025]. See the Terms and Conditions (https://onlinelibrary.wiley.com/terms-and-conditions) on Wiley Online Library for rules of use; OA arctices are governed by the applicable Creative Commons Licenses

15213773, 0. Downloaded from https://onlinelibrary.wilej.com/doi/10.1002/anie.202517656 by University Of Hawaii At Manoa, Wiley Online Library on [10/11/2025], See the Terms and Conditions (https://onlinelibrary.wilej.com/terms-and-conditions) on Wiley Online Library for rules of use; OA articles are governed by the applicable Creative Commons License

Figure 3. Potential energy surface of the reaction silicon nitride radical (SiN, $C_{\infty v}$, $X^2\Sigma^+$) and 1,3 butadiene (C_4H_6 , C_{2h} , X^1A_1) where dotted lines represent the doublet surface. The numbers denote energies (in kJ mol⁻¹) for each species calculated at the CCSD(T)-F12/cc-pVTZ-F12//B2PLYP-D3(BJ) /Def2-TZVPP + ZPE (B2PLYP-D3(BJ) /Def2-TZVPP) level of theory. Atoms are color-coded in purple (silicon), blue (nitrogen), grey (carbon), and white (hydrogen).

state to p2 (path b) can account for the experimental data. Although both the p1 and p2 product channels are accessible, the formation of p1 remains the overall lowestenergy pathway, consistent with its thermodynamic stability over p2. To identify the most favorable pathway, Rice-Ramsperger-Kassel-Marcus (RRKM) statistical analysis was performed (see Supporting Information). The results indicate that, under statistical conditions, p1 would be the dominant product, with a branching ratio of p1:p2:p3 = 88.1:2.6:9.3. RRKM calculations also indicate that the rate constant for the i3 \rightarrow i4 transition is approximately 10⁵ times slower than that for $i3 \rightarrow i5$ (Table S2), suggesting that the formation of p2 via dissociation of i4 contributes negligibly to the overall product distribution. Under these conditions, about 97% of the **i6** intermediate dissociates to **p1**, while only 3% leads to **p2**.

-350

Quasi-Atomic Orbital Analysis

Having identified novel azasilabenzenes, to better understand the chemical bonding of these SiNC₄H₅ isomers, a detailed quasi-atomic orbital (QUAO) analysis was performed at RHF//Def2-TZVPP//B2PLYP-D3(BJ)/Def2-TZVPP level of theory using GAMESS software. [62-64] The interference kinetic bond orders (KBOs) provide a quantitative measurement of the bond strength. Figure 4 displays the orbitals that participate in the π - π bonding interaction. For **p3**, the electron occupations of π QUAOs for Si (0.47) and N (1.47) imply a charge transfer from Si to N, which agrees well with the difference in electronegativity of the two atoms. The small variations between the occupations of C_{π} orbitals demonstrate a lower degree of charge polarization compared with Si-N π . For **p1** and **p2**, such transfer of charges from Si_{π} to N_{π} can be observed, while there is a higher degree of charge transfer among C_{π} orbitals compared with **p3**.

In agreement with QUAO analysis for C₂H₂ versus Si₂H₂ from Guidez, Gordon, and Ruedenberg that the lowering of interatomic KBO is the driving force of bond formation, the most stable isomer **p1** has the lowest interatomic KBO, followed by p2 and p3, respectively.^[65] The dominant KBOs are the σ interactions with an increase in the order of Si-C/N < C-C < C-N (Figure 4). These indicate that the C-N σ is the strongest, followed by C-C σ , while the Si-N and Si-C are the weakest σ interactions. The C-C bond distances of **p2** are ideally equivalent (140 pm), which align well with the slight difference in KBOs of C-C π interactions. Moreover, Table S4 demonstrates the weak interactions between the two C-C double bonds (KBO = -28 kJ mol^{-1}) and N_{π} and C_{π} QUAOs (KBO = -33 kJ mol^{-1}) of **p3**. Based on the theoretical studies, **p1** is more stable than **p2** by 25 kJ mol⁻¹. However, the stable form of their isovalent molecule, pyridine, is more favored to exhibit lone-paired electrons at N instead of an N-H bond due to aromaticity. Comparing **p1** and **p2**, the KBOs of their σ - σ and π - π interactions are in the same order of magnitude, except for N-H versus Si-H. The former has stronger bonding (KBO = -178 vs. -105 kJ mol⁻¹, respectively). This is likely due to a better orbital overlap between N and H atoms. Another reason for the stability of **p1** over **p2** attributes to the reduced sp hybridization of the silicon atom. In Table \$5, there are about 10%-20% of s-characters contributing to the $Si-\sigma$ -type QUAOs for **p1**, whereas one can see that those for p2 are greater (30%-35%). These imply that a high degree of sp mixing is unfavored for the silicon atom. This is in excellent agreement with the concept of sp hybridization in which it is more applicable for the second row of the periodic table, as the energy levels of 2s and 2p are closer to each other. Such sp mixing is less likely to be exhibited when going below the second period elements.

To characterize the degree of aromaticity of p1 and p2, the nucleus-independent chemical shielding (NICS)^[66,67] was

Research Article

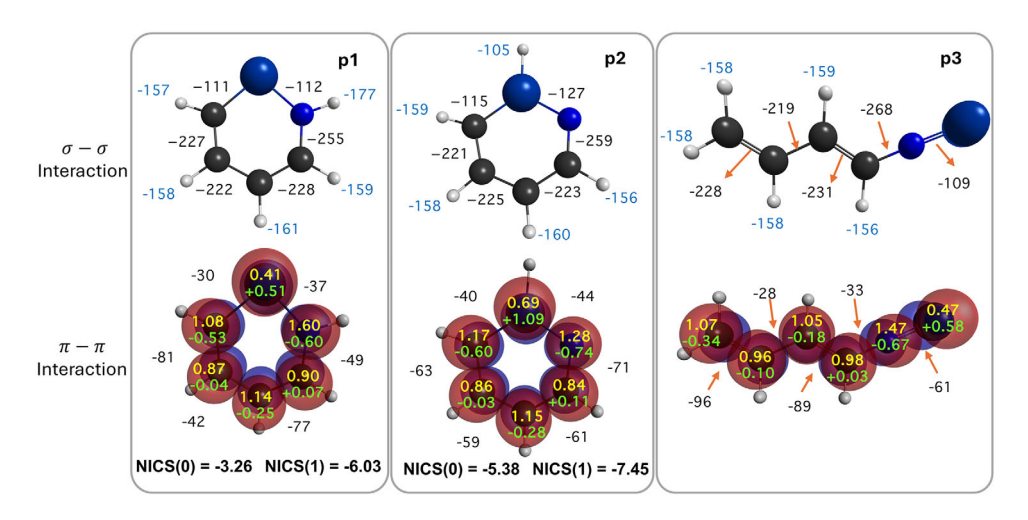


Figure 4. QUAOs analysis of p1, p2, and p3 calculated at RHF//B2PLYP/Def2-TZVPP level of theory. Black numbers represent KBO energies of E—E σ and π bonds with E = C, N, or Si, whereas blue is KBO energies of E—H σ bonds. Green indicates charge at each atom center. Yellow numbers are the electron populations in π QUAOs. NICS (0) and NICS (1) were calculated at B2PLYP/Def2-TZVPP level of theory.

calculated, as shown in Figure 4. Clearly, both NICS (0) and NICS (1) values of **p2** are more negative than those of **p1**, suggesting that **p2** has a higher aromatic character than **p1**. This also aligns well with the QUAO analysis. While the KBO energies and bond orders (BOs) of the π - π interactions (particularly C-C and C-N interactions) of **p2** are in the same range (KBO = -70 to -60 kJ mol⁻¹ and BO = 0.6-0.7), large deviations of the KBOs and BOs of **p1** can be observed (Figure 4 and Table S4). This indicates that the π electrons of **p1** are more localized than those of **p2**.

Conclusion

Our combined experimental and computational study demonstrates the gas-phase formation of two novel silicon-nitrogencarrying benzene isomers via a single-collision reaction between two acyclic precursors: the silicon nitride radical (SiN) and 1,3-butadiene (C₄H₆). The reaction initiates through a barrierless addition of the nitrogen atom to the π -electron density of the terminal carbon atom forming a nitrogen-carbon single bond. A subsequent trans-cis isomerization, followed by cyclization and multiple atomic hydrogen migrations, concludes with atomic hydrogen elimination. This sequence leads to the formation of two exotic silicon-nitrogen heterocyclic molecules through an overall indirect scattering mechanism: 1-aza-2-silacyclohexa-3,5dien-2-ylidene (SiC₄H₅N, X^1A' , **p1**) and 1-aza-2-silabenzene (SiC₄H₅N, X^1A' , **p2**). All transition states associated with the isomerization and product formation lie well below the energy of the separated reactants, indicating that the synthesis of these exotic cyclic molecules is feasible not only under high-temperature conditions but also in extremely low-temperature environments. Furthermore, we performed QUAO analysis to investigate the nature of chemical bonding and interatomic interactions in the synthesized products. The QUAO results reveal that the greater stability of the nonaromatic product **p1** compared to the aromatic **p2** attribute, in part, to a stronger N-H bonding interaction in p1 (KBO =-178 for N-H bond vs. -105 kJ mol⁻¹ for Si-H bond in **p2**) and a reduction in sp hybridization at the silicon center. The lower s-character observed in p1 (10%-20%) relative to p2 (30%-35%) further supports the notion that sp mixing is less favorable for third-row elements such as silicon. This study reveals the mechanistic pathway for synthesizing a previously unexplored class of organosilicon molecules. It is noteworthy that while the cyano radical (CN) is isovalent with the silicon nitride radical (SiN), it does not participate in a ring-closing reaction with 1,3-butadiene to eventually form pyridine; rather, it essentially produces an acyclic 1-cyano-1,3-butadiene derivative, unlike silicon nitride, which prefers cyclization reactions to access eventually azasilabenzenes. More broadly, while carbon and silicon are isovalent, both experimental and theoretical investigations at the molecular level demonstrate that they differ significantly in various aspects of reactivity and structural behavior.

Supporting Information

The authors have cited additional references within the Supporting Information. [68-82]

Acknowledgements

The experimental work at the University of Hawai'i at Manoa was supported by National Science Foundation (NSF) CHE 2244717. B.R.L.G. thanks Conselho Nacional de Desenvolvimento Científico e Tecnológico (CNPq), grant nos. 311508/2021–9 and 405524/2021–8. The technical support and advanced computing resources from University of Hawaii Information Technology Services – Research Cyberinfrastructure, funded in part by the National Science Foundation CC* awards #2201428 and #2232862 are gratefully acknowledged.

15213773, 0. Downloaded from https://oninelibarry.wile.com/doi/10.1002/anie.2025/7656 by University O' Hawaii At Manoa, Wiley Online Libarry on 10/11/2025]. See the Terms and Conditions (https://onlinelibrary.wiley.com/terms-and-conditions) on Wiley Online Libarry for rules of use; OA arctics are governed by the applicable Creative Commons Licenses

15213773, 0. Downloaded from https://onlinelibrary.wiley.com/doi/10.10102/anie.2023/17656 by University Of Hawaii At Manoa, Wiley Online Library on [10/11/2023]. See the Terms and Conditions (https://onlinelibrary.wiley.com/terms-and-conditions) on Wiley Online Library for rules of use; OA articles are governed by the applicable Creative Commons License



Conflict of Interests

The authors declare no conflict of interest.

Data Availability Statement

The data that support the findings of this study are available from the corresponding author upon reasonable request.

Keywords: Gas-phase reaction • Reaction dynamics • Silicon chemistry • Silicon substituted hydrocarbon • Silicon-nitrogen-containing heterocycle

- [1] J. A. Joule, *Heterocyclic Chemistry*, CRC Press, Florida 2020, https://doi.org/10.1201/9781003072850.
- [2] T. Kunieda, H. Matsunaga, Oxazoles: Synthesis, Reactions, and Spectroscopy, Vol. 60, 2004, pp. 1–52.
- [3] N. Tokitoh, K. Wakita, T. Matsumoto, T. Sasamori, R. Okazaki, N. Takagi, M. Kimura, S. Nagase, J. Chin. Chem. Soc. 2008, 55, 487–507, https://doi.org/10.1002/jccs.200800073.
- [4] E. G. Brown, Ring Nitrogen and Key Biomolecules: The Biochemistry of N-heterocycles, Springer Science & Business Media, Amsterdam 1998, https://doi.org/10.1007/978-94-011-4906-8.
- [5] A. F. Pozharskii, A. T. Soldatenkov, A. R. Katritzky, Heterocycles in Life and Society: An Introduction to Heterocyclic Chemistry, Biochemistry and Applications, John Wiley & Sons, New Jersey 2011, https://doi.org/10.1002/9781119998372.
- [6] M. M. Heravi, V. Zadsirjan, RSC Adv. 2020, 10, 44247–44311, https://doi.org/10.1039/D0RA09198G.
- [7] H. Stähle, Best Pract. Res. Clin. Anaesthesiol. 2000, 14, 237–246, https://doi.org/10.1053/bean.2000.0079.
- [8] J. Fischer, C. R. Ganellin, Chem. Int. 2010, 32, 12-15.
- [9] A. R. Massah, S. Gharaghani, H. A. Lordejani, N. Asakere, Med. Chem. Res. 2016, 25, 1538–1550, https://doi.org/10.1007/s00044-016-1585-z.
- [10] J. D. Watson, F. H. C. Crick, Clin. Orthop. Relat. Res. 2007, 462, 3–5, https://doi.org/10.1097/BLO.0b013e31814b9304.
- [11] I. Langmuir, J. Am. Chem. Soc. 1919, 41, 868–934, https://doi. org/10.1021/ja02227a002.
- [12] J. Chandrasekhar, P. v. R. Schleyer, R. Baumgaertner, M. T. Reetz, J. Org. Chem. 1983, 48, 3453–3457, https://doi.org/10. 1021/jo00168a016.
- [13] K. K. Baldridge, O. Uzan, J. M. Martin, Organometallics 2000, 19, 1477–1487, https://doi.org/10.1021/om9903745.
- [14] U. D. Priyakumar, D. Saravanan, G. N. Sastry, *Organometallics* 2002, 21, 4823–4832, https://doi.org/10.1021/om020419t.
- [15] R. Kinjo, M. Ichinohe, A. Sekiguchi, N. Takagi, M. Sumimoto, S. Nagase, J. Am. Chem. Soc. 2007, 129, 7766–7767, https://doi.org/10.1021/ja072759h.
- [16] T. Yang, B. B. Dangi, A. M. Thomas, B. J. Sun, T. J. Chou, A. H. Chang, R. I. Kaiser, *Angew. Chem.* 2016, 128, 8115–8119, https://doi.org/10.1002/ange.201602064.
- [17] A. M. Thomas, B. B. Dangi, T. Yang, R. I. Kaiser, B.-J. Sun, T.-J. Chou, A. H. H. Chang, *Chem. Phys.* 2019, 520, 70–80, https://doi. org/10.1016/j.chemphys.2019.01.001.
- [18] V. S. Krasnoukhov, V. N. Azyazov, A. M. Mebel, S. Doddipatla, Z. Yang, S. Goettl, R. I. Kaiser, *ChemPhysChem* 2021, 22, 1497– 1504, https://doi.org/10.1002/cphc.202100235.
- [19] M. R. Hoffmann, Y. Yoshioka, H. F. Schaefer III, J. Am. Chem. Soc. 1983, 105, 1084–1088, https://doi.org/10.1021/ja00343a002.

- [20] T. Lu, Q. Hao, J. J. Wilke, Y. Yamaguchi, D.-C. Fang, H. F. Schaefer III, J. Mol. Struct. 2012, 1009, 103–110, https://doi.org/10.1016/j.molstruc.2011.10.032.
- [21] B. T. Colegrove, H. F. I. Schaefer, J. Phys. Chem. 1990, 94, 5593–5602, https://doi.org/10.1021/j100377a036.
- [22] M. Lein, A. Krapp, G. Frenking, J. Am. Chem. Soc. 2005, 127, 6290–6299, https://doi.org/10.1021/ja042295c.
- [23] J. Y. Corey, in *Organic Silicon Compounds (1989)*, John Wiley & Sons, New Jersey 1989, pp. 1–56.
- [24] K. Wakita, N. Tokitoh, R. Okazaki, N. Takagi, S. Nagase, J. Am. Chem. Soc. 2000, 122, 5648–5649, https://doi.org/10.1021/ja000309i.
- [25] P. H. Blustin, J. Organomet. Chem. 1979, 166, 21–24, https://doi. org/10.1016/S0022-328X(00)91416-5.
- [26] F. Kleemiss, P. Puylaert, D. Duvinage, M. Fugel, K. Sugimoto, J. Beckmann, S. Grabowsky, Struct. Sci. 2021, 77, 892–905.
- [27] S. M. Sieburth, in *Designing Safer Chemicals*, Vol. 640, American Chemical Society, Washington, D.C 1996, pp. 74–83.
- [28] B. K. Hogendorp, Ph.D. thesis, University of Illinois at Urbana-Champaign (United States – Illinois), 2008.
- [29] S. J. Barraza, S. E. Denmark, J. Am. Chem. Soc. 2018, 140, 6668–6684, https://doi.org/10.1021/jacs.8b03187.
- [30] A. J. Arduengo III, R. L. Harlow, M. Kline, J. Am. Chem. Soc. 1991, 113, 361–363, https://doi.org/10.1021/ja00001a054.
- [31] M. Denk, R. Lennon, R. Hayashi, R. West, A. V. Belyakov, H. P. Verne, A. Haaland, M. Wagner, N. Metzler, J. Am. Chem. Soc. 1994, 116, 2691–2692, https://doi.org/10.1021/ja00085a088.
- [32] B. T. Luke, J. Pople, M. Krogh-Jespersen, Y. Apeloig, M. Karni, J. Chandrasekhar, P. v. R. Schleyer, J. Am. Chem. Soc. 1986, 108, 270–284, https://doi.org/10.1021/ja00262a014.
- [33] A. J. Arduengo III, H. Bock, H. Chen, M. Denk, D. A. Dixon, J. C. Green, W. A. Herrmann, N. L. Jones, M. Wagner, R. West, J. Am. Chem. Soc. 1994, 116, 6641–6649, https://doi.org/10.1021/ ia00094a020.
- [34] M. Haaf, T. A. Schmedake, R. West, Acc. Chem. Res. 2000, 33, 704–714, https://doi.org/10.1021/ar950192g.
- [35] N. J. Hill, R. West, J. Organomet. Chem. 2004, 689, 4165–4183, https://doi.org/10.1016/j.jorganchem.2004.09.012.
- [36] R. West, M. Denk, Pure Appl. Chem. 1996, 68, 785–788, https://doi.org/10.1351/pac199668040785.
- [37] M. Kassaee, H. Zandi, M. Momeni, F. Shakib, M. Ghambarian, J. Mol. Struct. THEOCHEM. 2009, 913, 16–21, https://doi.org/ 10.1016/j.theochem.2009.07.001.
- [38] T. Veszprémi, L. Nyulászi, T. Kárpáti, J. Phys. Chem. 1996, 100, 6262–6265, https://doi.org/10.1021/jp952810g.
- [39] L. Nyulászi, T. Karpati, T. Veszpremi, J. Am. Chem. Soc. 1994, 116, 7239–7242, https://doi.org/10.1021/ja00095a029.
- [40] C. Heinemann, W. A. Herrmann, W. Thiel, J. Organomet. Chem. 1994, 475, 73–84, https://doi.org/10.1016/0022-328X(94) 84009-1.
- [41] Y. Wang, J. I.-C. Wu, Q. Li, P. v. R. Schleyer, Org. Lett. 2010, 12, 4824–4827, https://doi.org/10.1021/ol102012d.
- [42] R. I. Kaiser, Chem. Rev. 2002, 102, 1309–1358, https://doi.org/10. 1021/cr970004v.
- [43] X. Gu, R. I. Kaiser, Acc. Chem. Res. 2009, 42, 290–302, https://doi.org/10.1021/ar8001365.
- [44] R. I. Kaiser, N. Balucani, Acc. Chem. Res. 2001, 34, 699–706, https://doi.org/10.1021/ar000112v.
- [45] Y. T. Lee, Angew. Chem., Int. Ed. 1987, 26, 939–951, https://doi. org/10.1002/anie.198709393.
- [46] S. B. Morales, C. J. Bennett, S. D. Le Picard, A. Canosa, I. R. Sims, B. Sun, P. Chen, A. H. Chang, V. V. Kislov, A. M. Mebel, *Astrophys. J.* 2011, 742, 26, https://doi.org/10.1088/0004-637X/742/1/26.
- [47] B. Sun, C. Huang, S. Chen, S. Chen, R. Kaiser, A. Chang, J. Phys. Chem. A 2014, 118, 7715–7724, https://doi.org/10.1021/ jp5056864.

Research Article



15213773, 0, Downloaded from https://onlinelibrary.wiley.com/doi/10.1002/anie.202517656 by University Of Hawaii At Manoa, Wiley Online Library on [10/11/2025]. See the Terms and Conditions (https://onlinelibrary.wiley.com/emrs/

-and-conditions) on Wiley Online Library for rules of use; OA articles are governed by the applicable Creative Commons License

- [48] D. R. Herschbach, Angew. Chem., Int. Ed. 1987, 26, 1221–1243, https://doi.org/10.1002/anie.198712211.
- [49] P. S. Weiss, in *Ph.D. Dissertation*, University of California, Berkeley, CA, 1986.
- [50] M. F. Vernon, Molecular Beam Scattering, University of California, Berkeley 1983.
- [51] R. D. Levine, Molecular Reaction Dynamics, Cambridge University Press, England 2009.
- [52] R. D. Levine, R. B. Bernstein, *Molecular Reaction Dynamics and Chemical Reactivity*, Oxford University Press, Oxford **1987**.
- [53] S. Grimme, J. Chem. Phys. 2006, 124, 034108, https://doi.org/10. 1063/1.2148954.
- [54] S. Grimme, S. Ehrlich, L. Goerigk, J. Comput. Chem. 2011, 32, 1456–1465, https://doi.org/10.1002/jcc.21759.
- [55] F. Weigend, R. Ahlrichs, Phys. Chem. Chem. Phys. 2005, 7, 3297, https://doi.org/10.1039/b508541a.
- [56] A. D. Becke, E. R. Johnson, J. Chem. Phys. 2005, 123, 154101, https://doi.org/10.1063/1.2065267.
- [57] F. Neese, WIREs Comput. Mol. Sci. 2022, 12, e1606, https://doi.org/10.1002/wcms.1606.
- [58] K. A. Peterson, T. B. Adler, H.-J. Werner, J. Chem. Phys. 2008, 128, 084102, https://doi.org/10.1063/1.2831537.
- [59] H. Werner, P. Knowles, G. Knizia, F. Manby, M. Schütz, P. Celani, W. Györffy, D. Kats, T. Korona, R. Lindh, MOLPRO, Version 2015.1, A Package of Ab Initio Programs, University of Cardiff Chemistry Consultants (UC3), Cardiff, Wales, UK 2015.
- [60] T. B. Adler, G. Knizia, H.-J. Werner, J. Chem. Phys. 2007, 127, 221106, https://doi.org/10.1063/1.2817618.
- [61] G. Knizia, T. B. Adler, H.-J. Werner, J. Chem. Phys. 2009, 130, 054104, https://doi.org/10.1063/1.3054300.
- [62] M. W. Schmidt, K. K. Baldridge, J. A. Boatz, S. T. Elbert, M. S. Gordon, J. H. Jensen, S. Koseki, N. Matsunaga, K. A. Nguyen, S. Su, J. Comput. Chem. 1993, 14, 1347–1363, https://doi.org/10.1002/jcc.540141112.
- [63] G. M. J. Barca, C. Bertoni, L. Carrington, D. Datta, N. De Silva, J. E. Deustua, D. G. Fedorov, J. R. Gour, A. O. Gunina, E. Guidez, T. Harville, S. Irle, J. Ivanic, K. Kowalski, S. S. Leang, H. Li, W. Li, J. J. Lutz, I. Magoulas, J. Mato, V. Mironov, H. Nakata, B. Q. Pham, P. Piecuch, D. Poole, S. R. Pruitt, A. P. Rendell, L. B. Roskop, K. Ruedenberg, T. Sattasathuchana, et al., J. Chem. Phys. 2020, 152, 154102, https://doi.org/10.1063/5.0005188.
- [64] F. Zahariev, P. Xu, B. M. Westheimer, S. Webb, J. Galvez Vallejo, A. Tiwari, V. Sundriyal, M. Sosonkina, J. Shen, G. Schoendorff, J. Chem. Theory Comput. 2023, 19, 7031–7055, https://doi.org/10. 1021/acs.jctc.3c00379.
- [65] E. B. Guidez, M. S. Gordon, K. Ruedenberg, J. Am. Chem. Soc. 2020, 142, 13729–13742, https://doi.org/10.1021/jacs.0c03082.
- [66] P. v. R. Schleyer, C. Maerker, A. Dransfeld, H. Jiao, N. J. R. van Eikema Hommes, J. Am. Chem. Soc. 1996, 118, 6317–6318, https://doi.org/10.1021/ja960582d.

- [67] Z. Chen, C. S. Wannere, C. Corminboeuf, R. Puchta, P. v. R. Schleyer, *Chem. Rev.* 2005, 105, 3842–3888, https://doi.org/10.1021/cr030088+.
- [68] R. I. Kaiser, P. Maksyutenko, C. Ennis, F. Zhang, X. Gu, S. P. Krishtal, A. M. Mebel, O. Kostko, M. Ahmed, Faraday Discuss. 2010, 147, 429, https://doi.org/10.1039/c003599h.
- [69] G. O. Brink, Rev. Sci. Instrum. 1966, 37, 857–860, https://doi.org/ 10.1063/1.1720347.
- [70] N. Daly, Rev. Sci. Instrum. 1960, 31, 264–267, https://doi.org/10. 1063/1.1716953.
- [71] A. C. West, J. J. Duchimaza-Heredia, M. S. Gordon, K. Ruedenberg, J. Phys. Chem. A 2017, 121, 8884–8898, https://doi. org/10.1021/acs.jpca.7b07054.
- [72] A. C. West, M. W. Schmidt, M. S. Gordon, K. Ruedenberg, J. Chem. Phys. 2013, 139, 234107, https://doi.org/10.1063/1. 4840776.
- [73] A. C. West, M. W. Schmidt, M. S. Gordon, K. Ruedenberg, J. Phys. Chem. A 2015, 119, 10360–10367, https://doi.org/10.1021/ acs.jpca.5b03399.
- [74] A. C. West, M. W. Schmidt, M. S. Gordon, K. Ruedenberg, J. Phys. Chem. A 2015, 119, 10368–10375, https://doi.org/10.1021/ acs.jpca.5b03400.
- [75] A. C. West, M. W. Schmidt, M. S. Gordon, K. Ruedenberg, J. Phys. Chem. A 2015, 119, 10376–10389, https://doi.org/10.1021/ acs.jpca.5b03402.
- [76] D. D. A. Cruz, K. N. Ferreras, T. Harville, G. Schoendorff, M. S. Gordon, *Phys. Chem. Chem. Phys.* **2024**, *26*, 21395–21406, https://doi.org/10.1039/D4CP01800A.
- [77] J. I. Steinfeld, J. S. Francisco, W. L. Hase, *Chemical Kinetics and Dynamics*, Vol. 2, Prentice Hall, Upper Saddle River, NJ 1999.
- [78] H. Eyring, S. H. Lin, Basic Chemical Kinetics, John Wiley & Sons, Inc., New Jersey 1980.
- [79] C. He, L. Zhao, A. M. Thomas, A. N. Morozov, A. M. Mebel, R. I. Kaiser, J. Phys. Chem. A 2019, 123, 5446–5462, https://doi.org/10.1021/acs.jpca.9b03746.
- [80] V. Kislov, T. Nguyen, A. Mebel, S. Lin, S. Smith, J. Chem. Phys. 2004, 120, 7008–7017, https://doi.org/10.1063/1.1676275.
- [81] G. L. Stoychev, A. A. Auer, F. Neese, J. Chem. Theory Comput. 2018, 14, 4756–4771, https://doi.org/10.1021/acs.jctc. 8b00624.
- [82] R. Ditchfield, Mol. Phys. 1974, 27, 789–807, https://doi.org/10. 1080/00268977400100711.

Manuscript received: August 11, 2025 Revised manuscript received: October 23, 2025 Manuscript accepted: October 24, 2025

Version of record online: ■■, ■